



“Gheorghe Asachi” Technical University of Iasi, Romania



PROMOTING EFFECT OF CERIA ON THE CATALYTIC ACTIVITY OF CeO₂-ZnO POLYCRYSTALLINE MATERIALS

Nicolae Apostolescu, Corina Cernătescu, Ramona-Elena Tătaru Fărnuș,
Claudia Cobzaru, Gabriela Antoaneta Apostolescu*

“Gheorghe Asachi” Technical University of Iasi, Faculty of Chemical Engineering and Environmental Protection,
73 Prof. Dr. docent Dimitrie Mangeron Str., 700050 Iasi, Romania

Abstract

A polycrystalline CeO₂-ZnO catalyst was prepared by using a hydrothermal procedure in order to improve the structural properties. This polycrystalline material was then used to remove organic pollutants from aqueous solutions by the means of photocatalysis. The structural, morphological and optical properties of as-prepared materials were characterized by several techniques, such as UV-visible spectroscopy, SEM, FTIR, XRD. The SEM analysis shows that the crystallite size sample varies in the range of 0.3-2 μm. The photocatalytic activity under UV irradiation was estimated by measuring the degradation rate of aqueous solutions of methylene blue (MB, 0.01mM/L) and 4'-(1-methyl-benzimidazolyl-2)-phenylazo-2''-(8''-amino-1''-hydroxy-3'', 6''-disulphonic)-naphthalene acid (PMBH, 0.05mM/L). The effect of catalyst content on the photocatalytic activity was also studied. The results confirm that this material can be potentially applied for the treatment of water contaminated by organic pollutants.

Key words: band gap energy, CeO₂-ZnO nanoparticles, photocatalytic degradation

Received: May, 2017; *Revised final:* February, 2018; *Accepted:* March, 2018; *Published in final edited form:* April 2018

1. Introduction

Recently, the need to keep the environment clean and safe has led to looking for efficient, and economically convenient solutions, such as semiconductor materials. Semiconductor materials have become particularly attractive to the scientific community, and are used in various fields, such as electronics, environmental remediation techniques (*i.e.* catalysts or photocatalysts (Favier et al., 2016; Fujishima and Zhang, 2006; Jesudoss et al., 2016; Nascimento et al., 2014; Paz, 2006; Reddy et al., 2015) or for conversion of solar energy (Bhosale et al., 2016; Fujishima and Honda, 1972; Lira-Cantu and Krebs, 2006).

Thus, when a semiconductor is irradiated with energy close to, or greater than the band gap energy (E_g), electrons are generated in the conduction band

(e^-) and holes in the valence band (h^+). These electric charges are mobile and are able to initiate various redox reactions on the surface of the catalyst, but they have the tendency to recombine quickly, thus dissipating the absorbed energy. Therefore, a semiconductor photocatalytic activity is dependent on the competition between the transfer of electric charge on its surface and recombination of electron-hole pairs (Faisal et al., 2013; Kaviyarasu et al., 2017). For many materials with the same chemical composition, the structural, catalytic and electronic properties may be completely different, depending on how these are processed (Jafari et al., 2016).

Zinc oxide and cerium (IV) oxide have been and still are intensively studied due to their versatility and multiple applications (Faisal et al., 2013; Nascimento et al., 2014). ZnO crystallizes in a hexagonal or cubic system, but the hexagonal form is

* Author to whom all correspondence should be addressed: e-mail: ganto@ch.tuiasi.ro

more stable. It is a semiconductor compound with the ionicity on the border between the ionic and covalent semiconductor. The chemical bond becomes partially ionic due to electronic charge transfer from Zn to O. In this way, the Coulomb interaction between the ions increases, hence the width of the band gap material also increases. One of its most important features is the polar surface that causes a series of specific properties, such as spontaneous polarization and piezoelectricity, leading to many applications in electronics, gas sensors or photocatalysis (Amira et al., 2017). ZnO is cheap, it can be recovered from waste products (Jule et al., 2016; Lopez et al., 2017) and has a low toxicity (Xia et al., 2008) being used as an ingredient in numerous products such as: drugs, cosmetics, photocatalyst, additive for textiles and paper (Atchudan et al., 2017; Faisal et al., 2013; Mirzaei and Darroudi, 2017). The properties of zinc oxide can be considerably improved by doping it with the various components such as transitional metal ions or oxides (Choi et al., 1994; Kannadasan et al., 2014; Lira-Cantu and Krebs, 2006; Mogensen et al., 2000). In the present paper, we focused on the study of a CeO₂-ZnO polycrystalline mixture.

2. Experimental

2.1. Material and methods

The chemicals used in this study were Zn(CH₃COO)₂ x2H₂O, Ce(NO₃)₃ x6H₂O, citric acid (all 99.99% purity, supplied from Sigma-Aldrich). The reagents were first dissolved in distilled water, and then mixed under vigorous stirring with the appropriate amounts of citric acid, at 333 K, for two hours, the obtained yellow precipitate was separated by decantation, then was washed and transferred into a furnace for 3 hours at 773 K, to remove the organic phase (Apostolescu et al., 2015). Other researchers have observed that Ce³⁺, heated over 773 K passes in Ce⁴⁺ (Nagy and Dekany, 2009). The yellow-white powders were used to establish the photocatalytic activity, without other treatments. Two samples were prepared, first named a1, starting from 1 mmol Ce(NO₃)₃ x6H₂O and 9 mmol Zn(CH₃COO)₂ x2H₂O and the second sample, named a2 starting from 3

mmol Ce(NO₃)₃ x6H₂O and 7 mmol Zn(CH₃COO)₂ x2H₂O.

The organic dyes tested were methylene blue-MB (Chemical Company) and 4'-(1-methylbenzimidazol-2-yl)-phenylazo-2''-(8''-amino-1''-hydroxy-3'',6''-disulphonic)-naphthalene acid abbreviated PMBH (synthesized in our laboratories) (Cernatescu et al., 2015) and are presented in Table 1.

2.2. Characterization methods

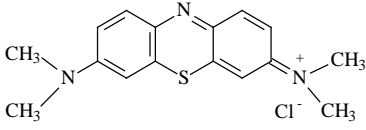
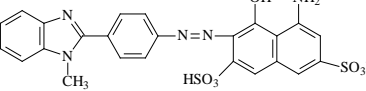
The phase composition of all powders and obtained samples were identified by the X-ray diffraction method (Philips PW 1840 diffractometer) under the following conditions: 40 kV, 30 mA, monochromatic CuK α radiation ($\lambda = 0.15418$ nm) over a 2θ range from 10 to 70°. The FTIR spectra were recorded on a Perkin Elmer Spectrum 100, resolution 2 cm⁻¹ using 32 scans in the range 4000 - 400 cm⁻¹; all samples were prepared as KBr pellets (ratio 5 / 95 wt.%). The morphology of prepared samples was observed by scanning electron microscope (Vega Tescan 30 kV). The ultraviolet-visible spectra were carried out using a spectrophotometer (UV-Vis SPECORD 200 Analytik Jena) for solid sample and SP 870plus METERTech for dyes residual concentration.

2.3. Photocatalysis experiments

Photocatalysis experiments were performed using an 18W Hg UV B lamp. The incident radiation intensity was measured as being 0.105 mW/cm², and was determined by a Hamamatsu C9536-01 meter with H9958 detector for 310 - 380 nm, scaled between 1 μ W/cm² and 100 mW/cm².

Samples containing the dyes (MB, 10⁻⁵ M, or PMBH, 5·10⁻⁵M, at natural pH), and 0.2 - 0.3 g/L photocatalytic materials were UV irradiated, and the concentration of the dye was monitored by UV-vis measurements (at 664 nm for MB and 540 nm for PMBH). Before recording the spectrum, the samples were centrifuged (5000 rotation/min) to separate the solid content. The dye-photocatalyst system was initially left for 30 minutes stirring in the dark, until adsorption equilibrium was reached.

Table 1. Characteristics of organic dye

Dye	Chemical structure	Molecular formula	λ_{max}	Molar mass
Methylene blue (MB)		C ₁₆ H ₁₈ ClN ₃ S	664 nm	319.85 g/mol
4'-(1-methylbenzimidazol-2-yl)-phenylazo-2''-(8''-amino-1''-hydroxy-3'',6''-disulphonic)-naphthalene acid (PMBH)		C ₂₄ H ₁₉ N ₅ O ₇ S ₂	540 nm	553 g/mol

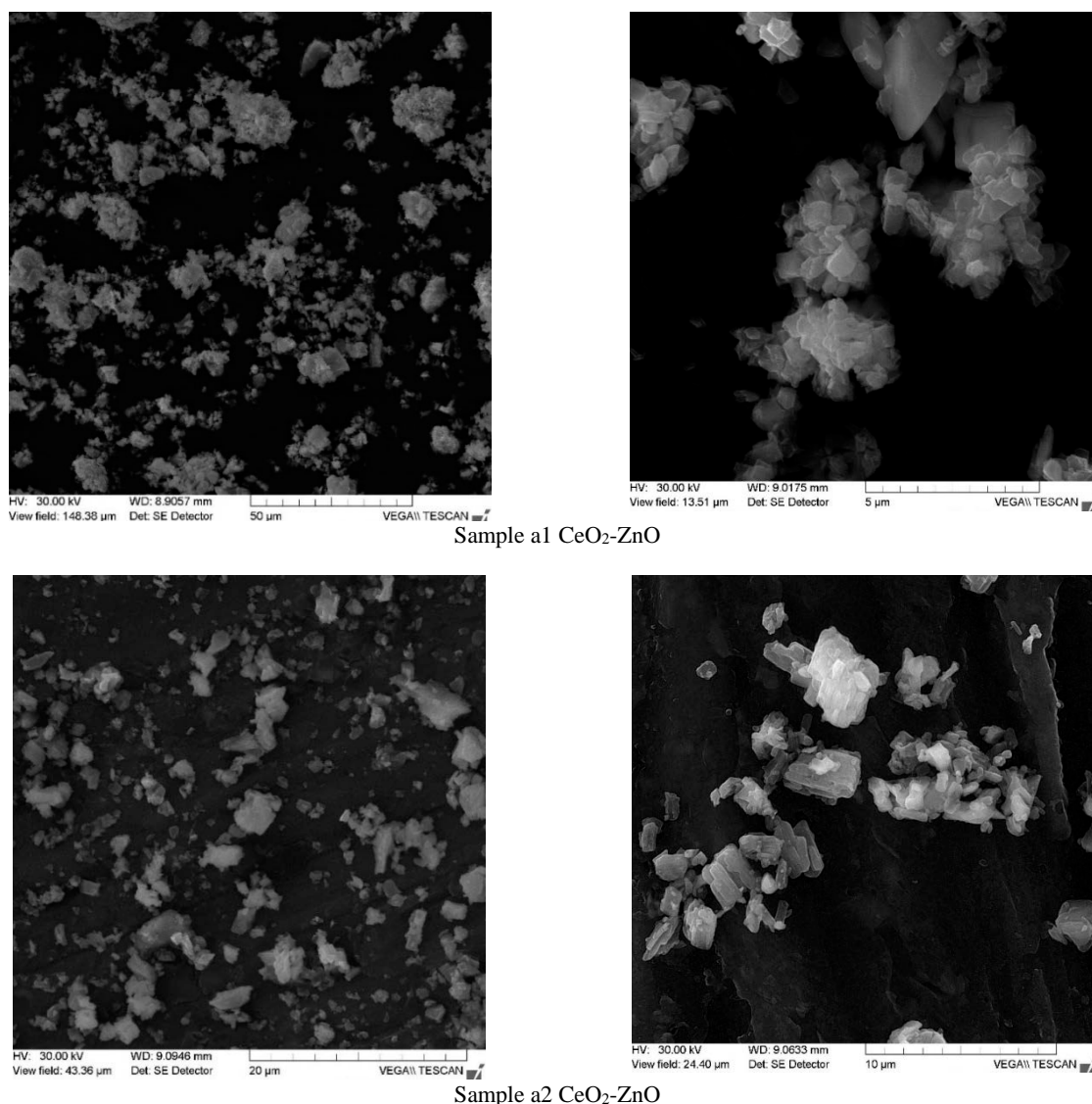


Fig. 1. SEM micrographs of a1 and a1 samples at different magnification

Degradation efficiency $D(\%)$, was calculated with Eq. (1):

$$D(\%) = \left[\frac{A(\text{dye})_i - A(\text{dye})_t}{A(\text{dye})_i} \right] \cdot 100 \quad (1)$$

where $A(\text{dye})_i$ and $A(\text{dye})_t$ are the absorbance of MB at 664 nm and PMBH at 540 nm, in the dark and under UV irradiation (at t minutes).

3. Results and discussion

3.1. Morphology and structure of CeO₂-ZnO photocatalysts

SEM micrograph of the surface morphology of CeO₂-ZnO prepared samples are shown in Fig. 1. Sample 1 with a low-CeO₂ content presents tabular aggregates, with size $0.3 \times 0.6 \mu\text{m}$ and $0.4 \times 0.7 \mu\text{m}$. The second sample shows prismatic aggregates ranging in size from $1 \times 0.5 \times 0.25 \mu\text{m}$ up to $2.5 \times 0.8 \times 0.3 \mu\text{m}$. The aggregates are actually composed of small CeO₂-ZnO

particles leading to a relatively rough surface. Microcrystals agglomeration is a common phenomenon, which tends to reach a state of minimum energy, by reducing the contact with the outside environment (Chen and Chang, 2006). The small size of crystallites reported is in accordance with determined photocatalytic activity.

UV-vis absorption spectra of the two samples is presented in Fig. 2, (inset), and were used to calculate the band gap energy, using the Tauc plot. According to the photocatalytic mechanism, the band gap of the semiconductor plays a major role in the photocatalytic activity of as-prepared materials. Band gap of the photocatalysts was determined through Eq. (2):

$$(ah\nu)^2 = k \cdot (h\nu - E_g) \quad (2)$$

where: $h\nu$ is the photon energy (eV), a is the absorption coefficient, k is a constant and E_g (eV) is the band gap energy. By extrapolating the linear region in a plot of $(ah\nu)^2$ versus photon energy, the

band gap can be estimated from graph, using Eq.(2). The band gap values are presented in Fig. 2 and have been found to be different than the value reported for bulk ZnO (3.3 eV) and CeO₂ (3.2 eV) due to quantum confinement, according to literature (Jha et al., 2013; Sabari Arul et al., 2015), the estimated band gap values for CeO₂-ZnO are 2.45eV and 2.7 eV.

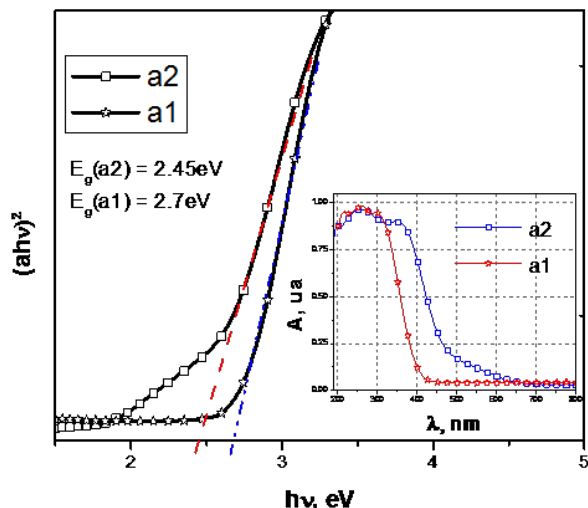


Fig. 2. The optical absorption energy band gap estimated for CeO₂-ZnO samples. Inset: the corresponding UV-vis absorption spectrum

FTIR analysis presented in Fig. 3 was performed in order to verify if during calcination, the organic phase left the system. It is observed that the characteristic peaks of the organic phase (1629-1590 cm⁻¹ corresponding to the carboxylic salt, 1310 cm⁻¹ alkyl bond and 796 cm⁻¹ C-H bonds) present in uncalcined samples are not found in the calcined samples. The Zn-O vibration is around 550 cm⁻¹, the large band located at 3400 - 3450 cm⁻¹ is attributed to the stretching vibration of O-H in the adsorbed water molecules (Khataee et al., 2015) and the Ce-O symmetric stretching vibration is around 520cm⁻¹ (Tambat et al., 2016).

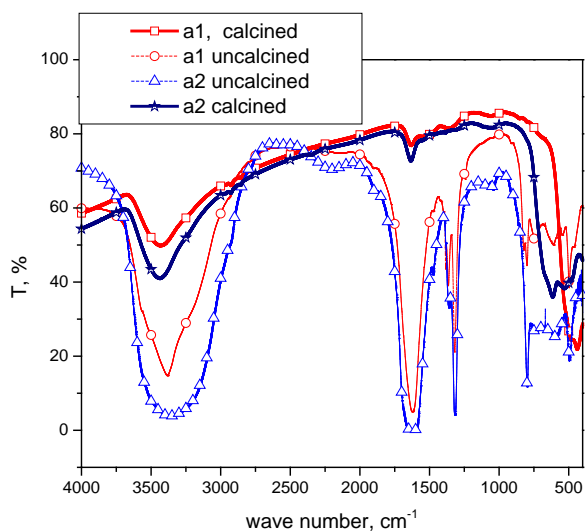


Fig. 3. FTIR analysis for sample a1 and a2 calcinated and uncalcinated

XRD patterns of CeO₂-ZnO composites are shown in Fig 4 and exhibits various peaks which could be indexed according to ZnO diffraction peaks (JCPDS card no. 36-1451) and CeO₂ diffraction peaks (JCPDS card no 34-0394): for CeO₂, the peaks presented at 2θ 28.5, 33.09, 47.49 and 56.4 can be indexed as (111), (200), (220) and (311) planes, and for ZnO the peaks presented at 2θ 31.9, 34.6, 36.4, 47.8 and 56.8 can be indexed as (100), (002), (101), (102), (110) (Jule et al., 2016; Sabari Arul et al., 2015). For the XRD pattern of the CeO₂-ZnO clearly matches with the polycrystalline structures of CeO₂ and ZnO, indicating the formation of composite CeO₂-ZnO without any other impurity.

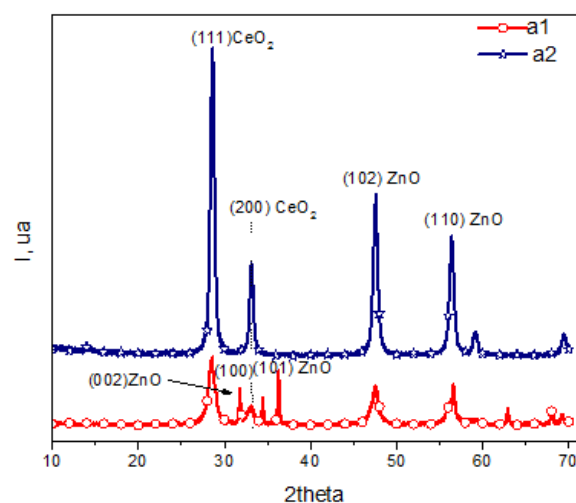


Fig. 4. The XRD patterns of CeO₂-ZnO composites

3.2. Photocatalytic activity

Photocatalytic activity of synthesized samples was evaluated by studying the behavior at UV irradiation of a cationic dye MB, and a diazoderivate, PMBH and are presented in Fig. 5 and Fig. 6. Blank experiments show that the two materials are stable at UV radiation.

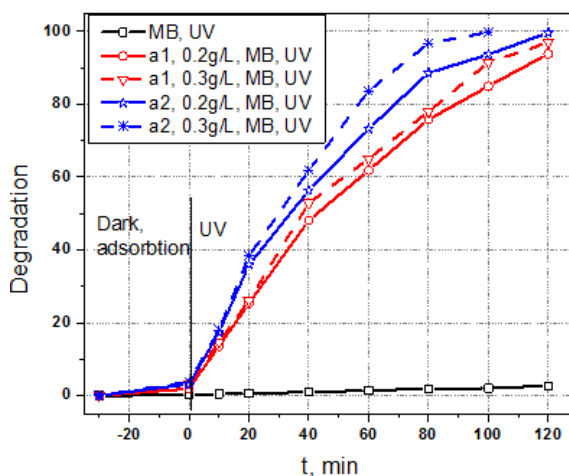


Fig. 5. Photocatalytic degradation rate of MB dye with CeO₂-ZnO prepared sample at different catalyst dose and under various UV-vis light irradiation times

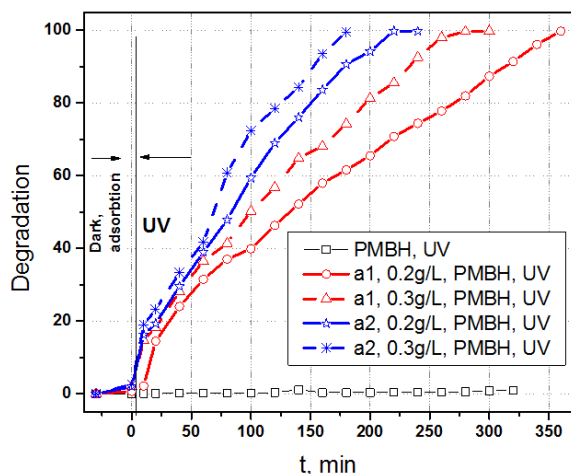
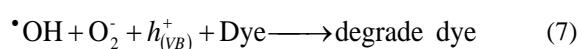
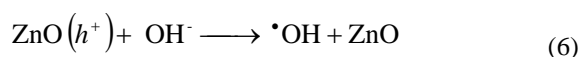
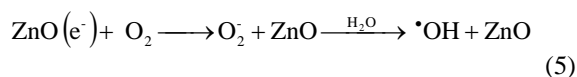
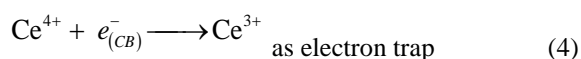
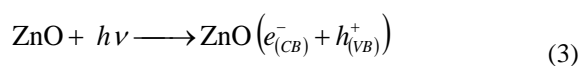


Fig. 6. Photocatalytic degradation rate of PMBH dye with CeO₂-ZnO prepared sample at different catalyst doses and under various UV-vis light irradiation times

After an hour of irradiation of the system (MB + sample a1), using 0.2 g/L catalyst concentration was achieved 60.5% as degree of discoloration and 63% for 0.3 g/L catalyst concentration. For sample a2 and after one hour of irradiation, the amount of discoloration varies from 73.4% for the dose of 0.2 g/L to 83.5% for 0.3 g/L catalyst. MB was discolored in a percentage of 97.6% after 80 minutes in the sample a2, 0.3 g/L.

When PMBH was used, the time was greater, compared with MB, so after 100 minutes for sample a1 was obtained a value of 39.8% for the dose of 0.2 g/L and 50% for the dose of 0.3 g/L and sample a2, 59.4% to 0.2 g/L and 72% to 0.3 g/L. A degree of discoloration by 99% was achieved after 180 minutes for sample a2, 0.3 g/L. Sample a1 (0.2 g/L) was completely degraded only after 360 minutes.

For the two dyes similar behavior was observed, such as increasing catalyst dose has resulted in a higher rate of degradation. The photocatalytic reactions describing the mechanism are shown in Eqs. (3 – 7), in agreement with the literature (Atchudan et al., 2017):



Also, the higher percentage of CeO₂ in the synthesized materials has led to higher rate of degradation, Ce⁴⁺ ions act as a trap to prevent recombination of electron-hole pairs created by

irradiation with ultraviolet radiation with $E > E_g$ (Lv et al., 2016), thus accelerating the photocatalytic process.

4. Conclusion

In this paper the synthesis, characterization and photocatalytic activity of two oxide materials based on CeO₂-ZnO are presented. The structure of materials synthesized by the hydrothermal process were investigated by SEM, FTIR, XRD, UV-vis and the band gap energy values were calculated.

The two catalytic materials are sensitive to low radiation doses, compared to those reported in the literature. Both samples show good photocatalytic activity measured for the degradation of PMBH and MB and the degree of discoloration of organic materials increased with the increasing percentage of CeO₂.

References

- Amira G., Chaker B., Habib E., (2017), Spectroscopic properties of Dy³⁺ doped ZnO for white luminescence applications, *Spectrochimica Acta Part A: Molecular and Biomolecular Spectroscopy*, **177**, 164-169.
- Apostolescu G.A., Cernatescu C., Cobzaru C., Tataru-Farmus R.E., Apostolescu N., (2015), Studies on the photocatalytic degradation of organic dyes using CeO₂ - ZnO mixed oxides, *Environmental Engineering and Management Journal*, **14**, 415-420.
- Atchudan R., Edison T.N.J.I., Perumal S., Shanmugam M., Lee Y.R., (2017), Direct solvothermal synthesis of zinc oxide nanoparticle decorated graphene oxide nanocomposite for efficient photodegradation of azo-dyes, *Journal of Photochemistry and Photobiology A: Chemistry*, **337**, 100-111.
- Bhosale R.R., Pujari S.R., Muley G.G., Patil S.H., Patil K.R., Shaikh M.F., Gambhire A.B., (2016), Solar photocatalytic degradation of methylene blue using doped TiO₂ nanoparticles, *Ceramics International*, **42**, 6728-6737.
- Cernatescu C., Apostolescu G.A., Cobzaru C., Tătaru-Fărmus R.E., Apostolescu N., Marinioiu A., (2015), Synthesis and physico-chemical behaviour studies for a new benzimidazole azodye, *Revue Roumaine de Chimie*, **60**, 837-844.
- Chen H.-I., Chang H.-Y., (2005), Synthesis of nanocrystalline cerium oxide particles by the precipitation method, *Ceramics International*, **31**, 795-802.
- Choi W., Termin A., Hoffmann M.R., (1994), The role of metal ion dopants in quantum-sized TiO₂: Correlation between photoreactivity and charge carrier recombination dynamics, *The Journal of Physical Chemistry*, **98**, 13669-13679.
- Faisal M., Ismail A.A., Ibrahim A., Bouzid H., Al-Sayari S.A., (2013), Highly efficient photocatalyst based on Ce doped ZnO nanorods: Controllable synthesis and enhanced photocatalytic activity, *Chemical Engineering Journal*, **229**, 225-233.
- Favier L., Simion A.I., Matei E., Grigoras C.G., Kadmi Y., Bouzaza A., (2016), Photocatalytic oxidation of a hazardous phenolic compound over TiO₂ in a batch system, *Environmental Engineering and Management Journal*, **15**, 1059-1067.

- Fujishima A., Honda K., (1972), Electrochemical photolysis of water at a semiconductor electrode, *Nature*, **238**, 37-38.
- Fujishima A., Zhang X., (2006), Titanium dioxide photocatalysis: present situation and future approaches, *Comptes Rendus Chimie*, **9**, 750-760.
- Jafari A.J., Dehghanifard E., Kalantary R.R., Gholami M., Esrafil A., Yari A.R., Baneshi M.M., (2016), Photocatalytic degradation of aniline in aqueous solution using ZnO nanoparticles, *Environmental Engineering and Management Journal*, **15**, 53-60.
- Jesudoss S.K., Judith Vijaya J., John Kennedy L., Iyyappa Rajan P., Al-Lohedan H.A., Jothi Ramalingam R., Kaviyarasu K., Bououdina M., (2016), Studies on the efficient dual performance of Mn_{1-x}Ni_xFe₂O₄ spinel nanoparticles in photodegradation and antibacterial activity, *Journal of Photochemistry and Photobiology B: Biology*, **165**, 121-132.
- Jha P.K., Gupta S.K., Lukacevic I., (2013), Electronic structure, photocatalytic properties and phonon dispersions of X-doped (X ¼ N, B and Pt) rutile TiO₂ from density functional theory, *Solid State Sciences*, **22**, 8-15.
- Jule L.T., Dejene F.B., Roro K.T., Urgessa Z.N., Both J.R., (2016), Rapid synthesis of blue emitting ZnO nanoparticles for fluorescent applications, *Physica B*, **497**, 71-77.
- Kannadasan N., Shanmugam N., Cholan S., Sathishkumar K., Viruthagiri G., Poonguzhali R., (2014), The effect of Ce⁴⁺ incorporation on structural, morphological and photocatalytic characters of ZnO nanoparticles, *Materials Characterization*, **97**, 37-46.
- Kaviyarasu K., Maria Magdalane C., Kanimozhi K., Kennedy J., Siddhardha B., Subba Reddy E., Rotte N.K., Sharma C.S., Thema F.T., Letsholathebe D., Mola G.T., Maaza M., (2017), Elucidation of photocatalysis, photoluminescence and antibacterial studies of ZnO thin films by spin coating method, *Journal of Photochemistry and Photobiology B: Biology*, **173**, 466-475.
- Khataee A., Karimi A., Arefi-Oskoui S., Soltani R.D.C., Hanifehpour Y., Soltani B., Joo S.W., (2015), Sonochemical synthesis of Pr-doped ZnO nanoparticles for sonocatalytic degradation of Acid Red 17, *Ultrasonics Sonochemistry*, **22**, 371-381.
- Lira-Cantu M., Krebs F.C., (2006), Hybrid solar cells based on MEH-PPV and thin film semiconductor oxides (TiO₂, Nb₂O₅, ZnO, CeO₂ and CeO₂-TiO₂): Performance improvement during long-time irradiation C.F., *Solar Energy Materials and Solar Cells*, **90**, 2076-2086.
- Lopez F.A., Cebriano T., García-Díaz I., Fernandez P., Rodríguez O., Lopez Fernandez A., (2017), Synthesis and microstructural properties of zinc oxide nanoparticles prepared by selective leaching of zinc from spent alkaline batteries using ammoniacal ammonium carbonate, *Journal of Cleaner Production*, **148**, 795-803.
- Lv Z., Zhong Q., Ou M., (2016), Utilizing peroxide as precursor for the synthesis of CeO₂/ZnO composite oxide with enhanced photocatalytic activity, *Applied Surface Science*, **376**, 91-96.
- Mirzaei H., Darroudi M., (2017), Zinc oxide nanoparticles: Biological synthesis and biomedical applications, *Ceramics International*, **43**, 907-914.
- Mogensen M., Sammes N.M., Tompsett G.A., (2000), Physical, chemical and electrochemical properties of pure and doped ceria, *Solid State Ionics*, **129**, 63-94.
- Nagy K., Dekany I., (2009), Preparation of nanosize cerium oxide particles in W/O microemulsions, *Colloids and Surfaces A: Physicochemical and Engineering Aspects*, **345**, 31-40.
- Nascimento L.F., Martins R.F., Silva R.F., Serra O.A., (2014), Catalytic combustion of soot over ceria-zinc mixed oxides catalysts supported onto cordierite, *Journal of Environmental Sciences*, **26**, 694-701.
- Paz Y., (2006), Preferential photodegradation - why and how?, *Comptes Rendus Chimie*, **9**, 774-787.
- Reddy D.A., Ma R., Kim T.K., (2015), Efficient photocatalytic degradation of methylene blue by heterostructured ZnO-RGO/RuO₂ nanocomposite under the simulated sunlight irradiation, *Ceramics International*, **4**, 6999-7009.
- Sabari Arul N., Mangalaraj D., Han I.J., (2015), Facile hydrothermal synthesis of CeO₂ nanopebbles, *Bulletin of Materials Science*, **38**, 1135-1139.
- Tambat S., Umale S., Sontakke S., (2016) Photocatalytic degradation of Milling Yellow dye using sol-gel synthesized CeO₂, *Materials Research Bulletin*, **76**, 466-472.
- Xia T., Kovochich M., Liong M., Madler L., Gilbert B., Shi H., Yeh J.I., Zink J.I., Nel A.E., (2008), Comparison of the mechanism of toxicity of zinc oxide and cerium oxide nanoparticles based on dissolution and oxidative stress properties, *American Chemical Society Nano*, **2**, 2121-2134.